

Modelling Faraday Screens in the Interstellar Medium*

Maik Wolleben and Wolfgang Reich

Max-Planck-Institut für Radioastronomie, Auf dem Hügel 69, 53121 Bonn, Germany

Abstract. Maps of Galactic polarized continuum emission at 1408, 1660, and 1713 MHz towards the local Taurus molecular cloud complex were made with the Effelsberg 100-m telescope. Minima in the polarized emission which are located at the boundary of a molecular cloud were detected. Beside high rotation measures and unusual spectral indices of the polarized intensity, these features are associated with the molecular gas. At the higher frequencies the minima get less distinct. We have modelled the multi-frequency observations by placing magneto-ionic Faraday screens at the distance of the molecular cloud. In this model Faraday rotated background emission adds to foreground emission towards these screens. The systematic variation of the observed properties is the result of different line-of-sight lengths through the screen assuming spherical symmetry. For a distance of 140 pc to the Taurus clouds the physical sizes of the Faraday screens are of the order of 2 pc. In this paper we describe the data calibration and modelling process for one such object. We find an intrinsic rotation measure of about -29 rad m^{-2} to model the observations. It is pointed out that the observed rotation measure differs from the physical. Further observational constraints from $\text{H}\alpha$ observations limit the thermal electron density to less than 0.8 cm^{-3} , and we conclude that the regular magnetic field strength parallel to the line-of-sight exceeds $20 \mu\text{G}$ to account for the intrinsic rotation measure.

1 Introduction

Various surveys of Galactic polarized emission revealed an unexpected richness in highly varying structures in the polarized sky as discussed on this conference. In many cases these fluctuations in the polarized intensity and position angle have no counterpart in total intensity. One likely explanation for these observations is polarized background emission modulated by Faraday rotation. However, many emitting and rotating layers may exist along the line-of-sight so that the observed polarization is a superposition of modified background and unmodified foreground emission layers.

The average density of thermal electrons in the Galactic plane is about 0.03 cm^{-3} and the average of the regular magnetic field along the line-of-sight is about 1 to $2 \mu\text{G}$ (Taylor & Cordes 1993, Gómez et al. 2001). However, local enhancements of n_e are often observed as diffuse H II -regions due to their optical $\text{H}\alpha$ emission occurring from ionization and recombination of hydrogen. At low observing frequencies Faraday rotation is high and the polarization angle of synchrotron radiation is very sensitive to fluctuations in the electron density. Other than $\text{H}\alpha$ emission Faraday rotation depends on electrons from all sorts of elements. Measurements of local conditions of the Galactic magnetic field are not straightforward and often done by exploiting the Zeeman splitting effect. Faraday rotation of polarized radiation is another tool for the investigation of magnetic fields in case the thermal electron density is known.

For a given observing frequency the amount of Faraday rotation is proportional to the product of the electron density times the magnetic field component parallel to the line-of-sight. Fluctuations in either or both lead to changes in the observed polarization angle. Since such fluctuations are often of small spatial extent, one can describe them in terms of Faraday screens. However, the observation of the effect of Faraday screens on polarized background radiation is not straightforward since foreground emission adds vectorially to the modified background. The closer the screen the more apparent its effect, and the key problem is the unknown distance of the Faraday screens. However, distances to the Taurus–Auriga molecular cloud complexes are known to be about $140 \pm 20 \text{ pc}$ (e.g. Elias 1978) and structures on pc–scales can be resolved with arcmin angular resolution. In addition the Taurus–Auriga

*Based on observations with the Effelsberg 100-m telescope operated by the Max-Planck-Institut für Radioastronomie (MPIfR), Bonn, Germany

complex is located at medium latitudes well below the Galactic plane resulting in a relatively short line-of-sight through the Galaxy.

Here, we analyze a map from the $\lambda 21$ cm *Effelsberg Medium Latitude Survey* (EMLS, see Reich et al., this volume), which shows a number of enhancements and depressions in the polarized intensity apparently related to molecular gas of the Taurus complex. We interpret the coincidence in position and shape as strong evidence for Faraday effects taking place at the distance of the molecular cloud. In order to derive physical properties of the associated Faraday screens we have complemented the $\lambda 21$ cm survey data of the Taurus–Auriga region by observations at 18 cm wavelength. We modelled the polarization data in order to constrain the physical parameters of the Faraday screens by taking foreground and background emission into account.

2 Observation and Calibration

The $\lambda 21$ cm EMLS covers the northern Galactic plane in the range of $|b| \leq 20^\circ$ at a frequency of 1.4 GHz. Follow-up observations of a field north of the center of the Taurus molecular cloud complex were carried out at 1660 and 1713 MHz. Total intensities and linear polarization were measured simultaneously with sensitivities of 15 mK (1408 MHz) to 19 mK (1713 MHz) for Stokes I and 8 mK (1408 MHz) to 10 mK (1713 MHz) for Stokes U and Q at angular resolutions of $9'.35$ (1408 MHz) to $7'.87$ (1713 MHz). The same receiver was used for all three frequencies, but different HF-filters were selected to suppress interferences. The effective bandwidth was 20 MHz for 1408 MHz and 14 MHz for 1660 and 1713 MHz. Fields were mapped two times in orthogonal scanning directions and are fully sampled. 3C 286 served as the main calibrator for total power and polarization data.

Varying ground and atmospheric radiation causes temperature gradients across the map. In order to remove such gradients a linear baseline is subtracted from each subscan. This procedure also removes real sky signals of large extent, which leads to a similar problem like missing zero spacings in synthesis telescope imaging. At 1408 MHz the missing large-scale emission is usually recovered by absolutely calibrated data. For total intensities 1.4 GHz data from the Stockert northern-sky survey (Reich 1982, Reich & Reich 1986) were used. For polarization data we rely so far on the Dwingeloo survey (Brouw & Spoelstra 1976). The final calibration of polarization will be made with the data from the new DRAO 1.4 GHz survey (see Wolleben et al., this volume). Therefore all quantitative results given below should be taken as preliminary. However, other than at 1.4 GHz there exist no absolutely calibrated surveys at 1660 or 1713 MHz and we calibrated the maps in the following way: The temperature spectral index β ($T \propto \nu^\beta$) of Galactic continuum emission was adopted to be $\beta = -2.7$ in the Taurus area (Reich & Reich 1988). We assumed the same spectral index also for the large-scale polarized intensity and calculated an average offset for the 1660 and 1713 MHz maps from the 1408 MHz map. Rotation measures across the Taurus region were determined by Spoelstra (1972) and are very low everywhere varying around zero, and therefore we assumed no position angle difference for the large-scale emission.

The total power maps for all three frequencies show smooth diffuse emission varying mainly with Galactic latitude and a large number of unrelated extragalactic sources, but no structures related to the polarized emission. However, there are numerous small-scale polarization minima obviously related to the molecular gas cloud (see Fig. 1). They show rather clear differences in intensity and polarization angle distribution between 1408 and 1713 MHz. Polarized intensities towards these minima increase at higher frequencies, which is in contrast to the large-scale polarized emission and other obviously unrelated small-scale variations. The variation of the polarization angle with frequency reveals rotations measures of up to 50 rad m^{-2} (see Fig. 2). The 1660 MHz data were used mainly for a consistency check of the modelling as described below.

3 Modelling a Faraday Screen

We have applied a simple model to describe the observed variations in the polarization maps at all three frequencies. In this model, a Faraday screen is modulating background polarized emission passing through it, which adds to a constant foreground emission. The foreground and background emission

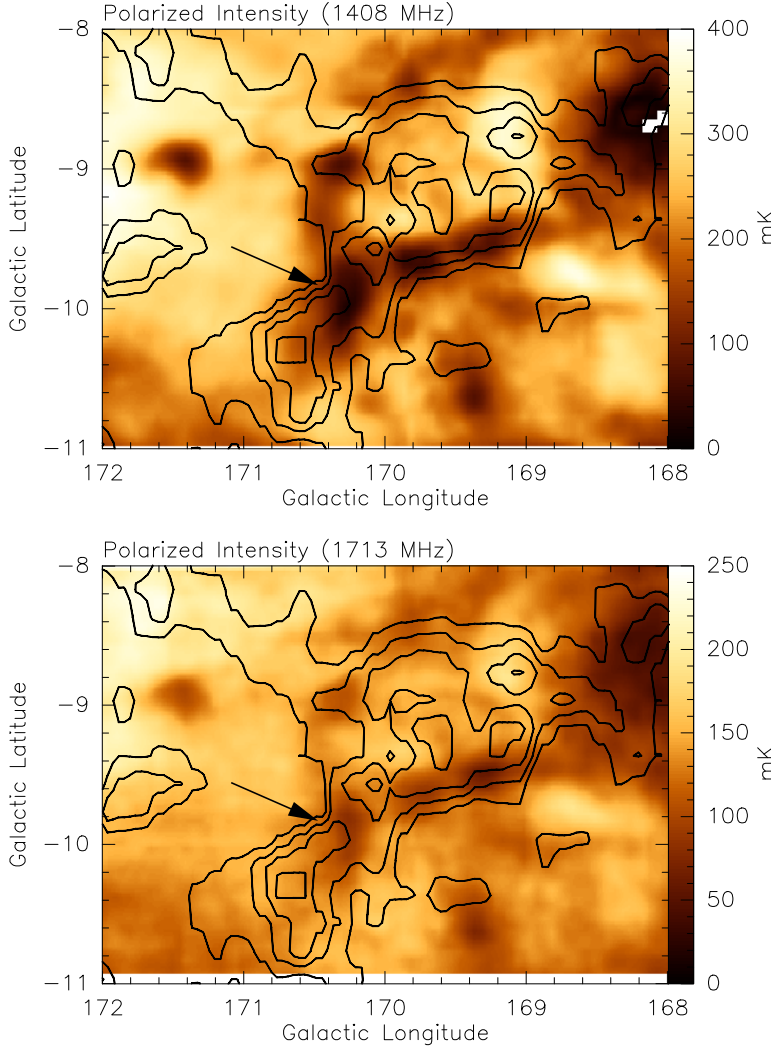


Fig. 1. Maps of the polarized intensity at 1408 (top) and 1713 MHz (bottom) towards a $4 \times 3^\circ$ region north of the center of the Taurus molecular cloud complex. Contours indicate the intensity of the velocity-integrated brightness temperature of $^{12}\text{CO}(1-0)$ emission (Dame et al. 2001). Contour levels are from 9 to 50 K km s^{-1} in steps of 3 K km s^{-1} . The minimum in the polarized intensity modelled as a Faraday screen in Sect. 3 is marked.

is assumed to be constant for all lines-of-sight through the Faraday screen. This seems justified since variations of polarized emission outside the Faraday screens are on larger scales.

At first we define a Faraday screen as an object which can affect the position angle and polarized intensity of polarized background radiation. The effect of the screen will depend on the path length radiation has to pass through it and thus depends on its size and shape. For reasons of simplicity we assume Faraday screens to be spherical objects with constant electron density, homogeneous magnetic field, and radius R . In case of elliptically shaped objects, coordinates were transformed to allow modelling in circular coordinates. The path length through the screen will therefore vary systematically with the observed position. With r as the distance from the center of the screen projected on the sky, the path length L is then given by $L(r) = 2R \cdot (1 - \frac{r^2}{R^2})^{1/2}$ and the fractional path length $l(r) = \frac{L(r)}{2R}$.

A Faraday screen may decrease the degree of polarization by beam depolarization, which seems possible due to the relatively small spatial extent of the Faraday screens discussed here. We assume any depolarization to increase linearly with the fractional path length $l(r)$ and express $DP_{\text{screen}}(r)$ by:

$$DP_{\text{screen}}(r) = l(r) \cdot (1 - DP_0) + DP_0 \quad (1)$$

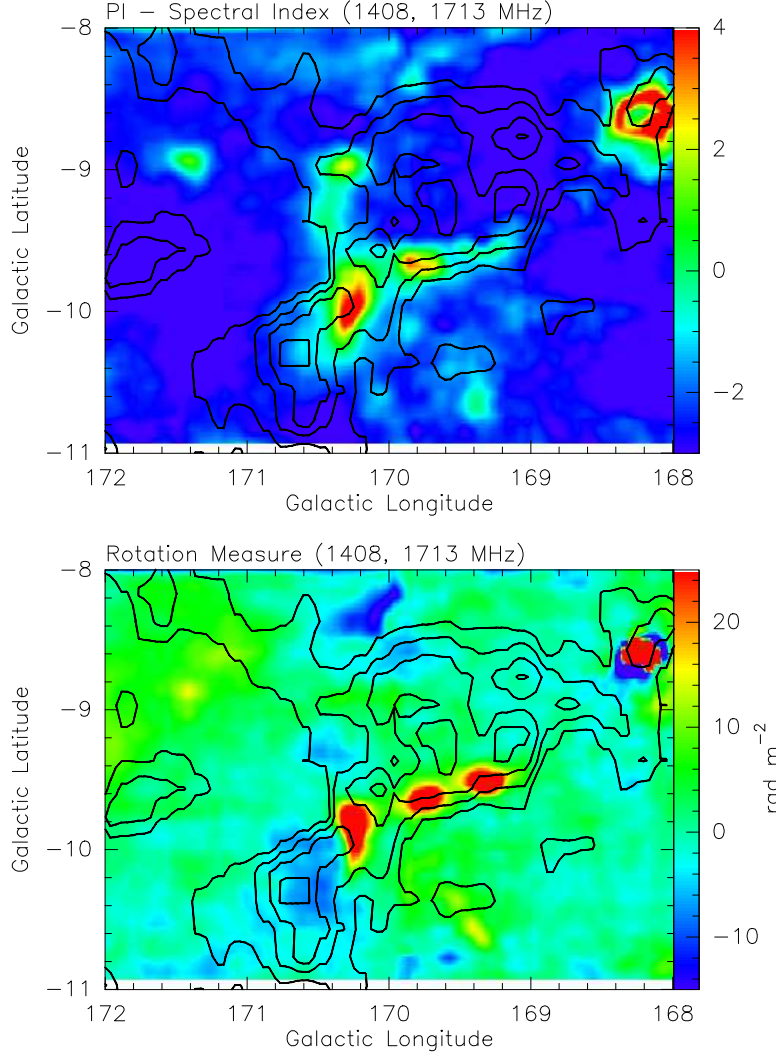


Fig. 2. Maps show the spectral index distribution of the polarized intensity (top) and the rotation measure distribution derived from the polarization angle rotation between 1408 and 1713 MHz (bottom). Contours are the same as in Fig. 1.

with DP_0 the maximum intrinsic depolarization at $r = 0$. In this notation $DP = 1$ means no depolarization and $DP = 0$ complete depolarization of the background radiation.

A Faraday screen also rotates the position angle of linearly polarized background radiation. The amount of Faraday rotation is given by $\Delta PA = RM \cdot \lambda^2$ with the rotation measure RM (rad m^{-2}) = $0.81 B_{\parallel} (\mu\text{G}) n_e (\text{cm}^{-3}) l$ (pc). The rotation measure of the screen depends on the fractional path length $l(r)$ and can be expressed as follows:

$$RM_{\text{screen}}(r) = RM_0 \cdot l(r) \quad (2)$$

with RM_0 the maximum intrinsic rotation measure at $r = 0$.

Depolarization and Faraday rotation are the two effects a Faraday screen might cause. The background polarized emission gets modified in a systematic way as a function of r and can be expressed by:

$$\begin{aligned} PI_{\text{mod}}(r) &= DP_{\text{screen}}(r) \cdot PI_{\text{back}} \\ PA_{\text{mod}}(r) &= RM_{\text{screen}}(r) \cdot \lambda^2 + PA_{\text{back}} \end{aligned} \quad (3)$$

The observed polarization is the superposition of the modified background and the foreground polarization, which in that case is a vector rather than a scalar addition as in the case of total

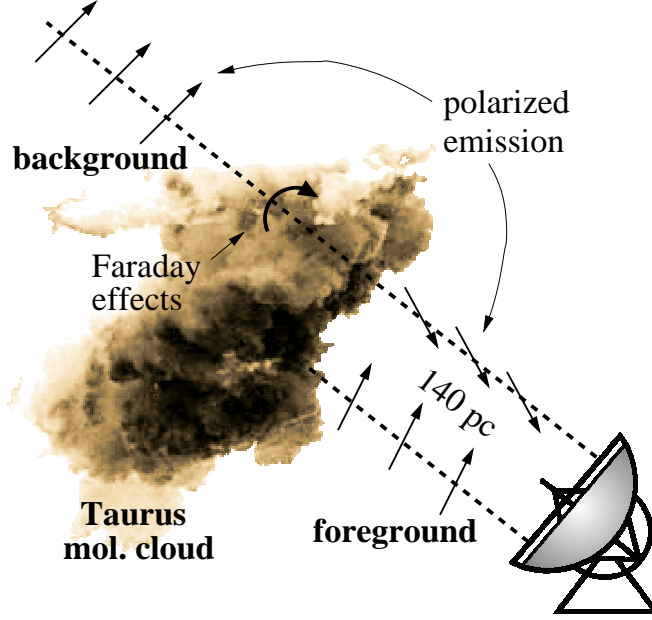


Fig. 3. Sketch of a Faraday screen showing the configuration of foreground and background polarized emission. Here, the Faraday screen is located at the surface of a molecular cloud. The observer measures the superposition of polarized emission from an unmodified foreground and a Faraday rotated and possibly depolarized background. The distance to the Taurus molecular clouds is 140 pc.

intensities. This means to add U and Q and calculate from these values the resulting PI and PA . With

$$\begin{aligned} U_{\text{mod}}(r) &= PI_{\text{mod}}(r) \cdot \sin(2PA_{\text{mod}}(r)) \\ Q_{\text{mod}}(r) &= PI_{\text{mod}}(r) \cdot \cos(2PA_{\text{mod}}(r)) \end{aligned} \quad (4)$$

The observable polarization calculates then by:

$$\begin{aligned} PI_{\text{obs}}(r) &= \sqrt{(U_{\text{fore}} + U_{\text{mod}}(r))^2 + (Q_{\text{fore}} + Q_{\text{mod}}(r))^2} \\ PA_{\text{obs}}(r) &= \frac{1}{2} \arctan \left(\frac{U_{\text{fore}} + U_{\text{mod}}(r)}{Q_{\text{fore}} + Q_{\text{mod}}(r)} \right). \end{aligned} \quad (5)$$

Fitting the two modelled observables PI_{obs} and PA_{obs} to the measured polarized intensities and angles towards the Faraday screens is done by optimizing the four free parameters of the model: PI_{fore} , PA_{fore} , RM_0 , and DP_0 . At $r \geq 1$ the pure superposition of background and foreground polarization must result in the measured polarization outside the screen. This limiting condition constrains the background polarization for $r < 1$. The model correctly reproduces the observed high spectral indices of polarized intensities, the rotation measures, as well as the observed variation in polarized intensity and angle (see Fig. 4). We find the following best-fit parameters for the Faraday screen marked in Fig. 1: $PI_{\text{fore}} \sim 150$ mK, $PA_{\text{fore}} \sim -1^\circ$, $PI_{\text{back}} \sim 130$ mK, $PA_{\text{back}} \sim -14^\circ$, $RM_0 \sim -29.3$ rad m $^{-2}$, and $DP_0 = 1$. These values describe the foreground and background emission, as well as the rotation measure (see next paragraph) and depolarization at 1.4 GHz. The other Faraday screens which can be identified will be discussed in a subsequent paper (Wolleben & Reich 2004).

Limitations of this model arise from the simplification of the shape and properties of Faraday screens, which are likely not perfectly elliptical with constant electron density and homogeneous magnetic field inside, but might be more turbulent or have a small filling factor. However, the absence of depolarization indicates little turbulence within the Faraday screen. Another simplification is that shape and size of the screens were estimated by eyeball based on their appearance in the PI-spectral index map. Finally, Faraday screens can overlap, which was not accounted for, but which is probably the case for the screen fitted here as seen from Fig. 1.

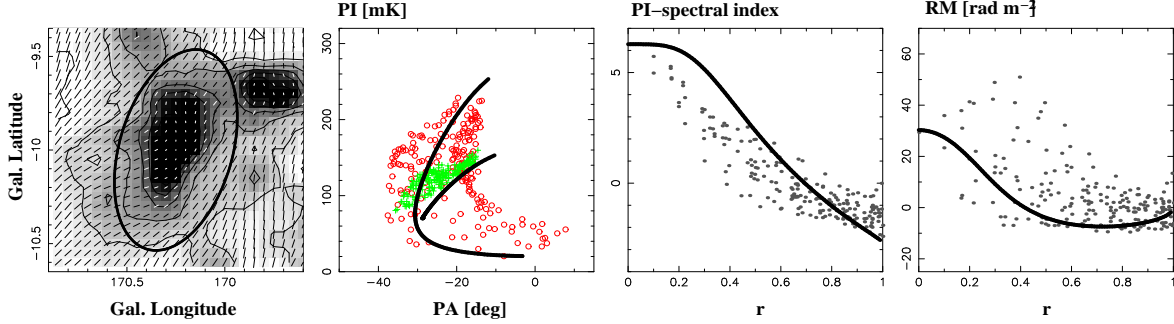


Fig. 4. From left to right are shown: map of the observed spectral index of polarized emission with an ellipse marking the size of the Faraday screen, the $PA-PI$ plot for 1408 MHz (red) and 1713 MHz (green), the observed spectral index of polarized emission, as well as the observed rotation measure versus radius r . The black lines indicate the model-fit.

4 Conclusions

Since the Faraday screen we observed towards the Taurus–Auriga molecular cloud complex is most likely associated with the molecular gas, we can specify its distance to 140 pc. When spherical symmetry is assumed, the size of the screen is of the order of 2 pc. An intrinsic RM of about -29 rad m^{-2} requires an excessive value for the thermal electron density or an excessive regular magnetic field component parallel to the line-of-sight, when compared to average Galactic values. The total power maps show no enhanced thermal emission at 1408, 1660, or 1713 MHz towards the Faraday screen which gives an upper limit for the thermal electron density of $n_e \leq 2 \text{ cm}^{-3}$. In addition, we have checked available $H\alpha$ data from the *full-sky H-alpha map* constructed by Finkbeiner (2003). No enhanced emission (at the 1σ detection level of 0.52 Rayleigh) related to the molecular gas or the Faraday screens is visible, which constrains n_e to less than 0.8 cm^{-3} for electrons from hydrogen ionization. With these upper limits for the thermal electron density a regular magnetic field strength exceeding $20 \mu\text{G}$ along the line-of-sight is needed to explain the intrinsic RM .

Towards the Faraday screen modelled here, the observed rotation measure RM_{obs} differs from its intrinsic rotation measure RM_{int} by about 60 rad m^{-2} and the sign of the observed RM s is in opposite direction. In the presence of foreground polarization, which adds to the Faraday rotated background, the observed RM is not a fixed value, but depends on the two frequencies used for its determination and in addition on the amount of foreground polarization adding to the rotated background. This implies no λ^2 -dependence of the observed polarization angles in the direction of Faraday screens.

References

- Brouw W. N., Spoelstra T. A. Th. (1976) *Astron. Astrophys. Suppl.* **26**, 129.
 Dame T. M., Hartmann D., Thaddeus P. (2001) *Astrophys. J.* **547**, 792.
 Elias J. H. (1978) *Astrophys. J.* **224**, 857.
 Finkbeiner D. P. (2003) *Astrophys. J. Suppl.* **146**, 407.
 Gómez G. C., Benjamin R. A., Cox, D. P. (2001) *Astron. J.* **122**, 908.
 Reich P., Reich W. (1986) *Astron. Astrophys. Suppl.* **63**, 205.
 Reich P., Reich W. (1988) *Astron. Astrophys.* **74**, 7.
 Reich W. (1982) *Astron. Astrophys. Suppl.* **48**, 219.
 Spoelstra T. T. Th. (1972) *Astron. Astrophys.* **21**, 61.
 Taylor J. H., Cordes J. M. (1993) *Astrophys. J.* **411**, 674.
 Wolleben M., Reich W. (2004) *Astron. Astrophys.*, submitted.